Surface and waveguide Josephson plasma waves in slabs of layered superconductors

T. M. Slipchenko,[1] D. V. Kadygrob,[2] D. Bogdanis,[3] V. A. Yampol'skii,[1,3,4] and A. A. Krokhin[5]

[1]*A.Ya. Usikov Institute for Radiophysics and Electronics, National Academy of Sciences of Ukraine, 61085 Kharkov, Ukraine*

[2]*Department of Microtechnology and Nanoscience, MC2, Chalmers University of Technology, SE-41296 Gothenburg, Sweden*

[3]*V.N. Karazin Kharkov National University, 61077 Kharkov, Ukraine*

[4]*The Abdus Salam International Centre for Theoretical Physics, I-34151 Trieste, Italy*

[5]*University of North Texas, 1155 Union Circle No. 311427, Denton, Texas 76203, USA*

(Received 30 August 2011; revised manuscript received 23 November 2011; published 20 December 2011)

We discuss the propagation of symmetric and antisymmetric Josephson plasma waves in a slab of layered superconductor clad between two identical dielectrics. We predict two branches of surface waves in the terahertz frequency range, one above and another below the Josephson plasma frequency. Apart from this, there exists a discrete set of waveguide modes with electromagnetic fields oscillating across the slab thickness and decaying exponentially away from the slab. We consider the excitation of the predicted waves by means of the attenuated-total-reflection method. It is shown that for a specific set of the parameters of the structure, the excitation of the waveguide modes is accompanied by the total suppression of specular reflection.

DOI: 10.1103/PhysRevB.84.224512 PACS number(s): 74.72.−h, 74.50.+r, 74.78.−w, 74.25.Gz

I. INTRODUCTION

The interaction of light with inhomogeneous metallic structures gives rise to many interesting effects. A well-known example is the Wood anomalies in light reflection from a periodic metal grating. A more recent example is the extraordinary transmission of light through metal films perforated by subwavelength holes.[1] The observed transmission coefficient turned out to be much larger than that predicted by Bethe's theory of electromagnetic diffraction at small apertures.[2] The enhancement of light transmission is related to the coupling of surface plasmons resonantly excited at both sides of the perforated film. A discussion of this and some alternative mechanisms of extraordinary transmission can be found in the review by Zayats *et al.*[3] The excitation of surface plasmons may also lead to an inverse effect of resonant suppression of light transmission through perforated metal films with thickness less than the skin depth.[4] The latter effect is accompanied by abnormal absorption of electromagnetic energy. Recent interest in the aforementioned anomalies is due to their possible applications for light control, photovoltaics, and the detection and filtering of radiation in visible and far-infrared frequency ranges.

It would be very desirable to have the ability to control the electromagnetic radiation also in the terahertz frequency range. Due to promising and important applications, the mastering of this frequency range (0.3–10 THz) is a new and rapidly developing area of research. Recently, a new approach for the waveguiding of THz waves has been proposed in Refs. 5–9 that uses structured metals (for instance, a set of metallic wires with diameter of about 1 mm) or an arrangement of subwavelength holes in a film of stainless steel. However, such metallic waveguides have a serious disadvantage. Indeed, since the terahertz frequencies are well below the frequency of surface-plasmon resonance, the extension of the terahertz waves away from the metallic waveguides significantly exceeds the wavelength.[10] Therefore, an essential part of the electromagnetic energy flows out of the waveguide, leading to strong radiation losses. To overcome this disadvantage, new materials, such as layered superconductors, are being considered for the design of the THz waveguides instead of metals.

Layered superconductors are either artificially grown stacks of Josephson junctions, such as Nb/Al-AlO_x/Nb, or natural high-temperature superconductors, such as $Bi_2Sr_2CaCu_2O_{8+\delta}$. These materials contain quite thin superconducting layers separated by thicker dielectrics. Many experiments on the **c**-axis transport in layered superconductors justify the use of a theoretical model in which the superconducting layers are coupled by the intrinsic Josephson effect through the layers (see, e.g., Refs. 11 and 12). Due to the layered structure, these superconductors possess strongly anisotropic current capability. Anisotropy here has a qualitative character: not only are the values of the in-plane and out-of-plane critical current densities strongly distinct, but even the nature of these currents is quite different. The origin of the in-plane current is the same as in bulk homogeneous superconductors and it can be described, for instance, in the local London limit. In contrast, the out-of-plane current is due to the Josephson effect. Because of strong anisotropy, the layered superconductors exhibit a wide variety of interesting physical properties.

The multilayered structure of $Bi_2Sr_2CaCu_2O_{8+\delta}$ (and similar superconductors) supports the propagation of specific Josephson plasma electromagnetic waves (JPWs) (see, e.g., review 13 and Refs. 14–21). For *infinite* layered superconductors, the spectrum of JPWs lies above the so-called Josephson plasma frequency ω_J. Possible applications of layered superconductors are related to the fact that ω_J belongs to the terahertz frequency range. In a *semi-infinite* sample, apart from the bulk JPWs, surface Josephson plasma waves (SJPWs) can propagate along the interface between the external dielectric and layered superconductor. As shown in Refs. 22–27, the spectrum of SJPWs also lies in the terahertz range and consists of two branches, one above ω_J and the other below it. These waves are similar to the surface-plasmon polaritons in normal metals. Thus, in analogy with normal metals, we expect that the resonance electromagnetic effects, in particular, the extraordinary transmission of terahertz signals, can exist

in slabs of layered superconductor due to the excitation of SJPWs.

The first step in the study of the effect of extraordinary transmission is the calculation of the spectrum of the SJPWs in a *finite-thickness* slab of layered superconductors. The properties of collective modes in layered superconductors have been a field of interest since the 1990s. The collective modes were studied in the limits of infinite,[14–21] extremely small,[28–30] and arbitrary[31,32] slab thickness. However, there exist only a few publications[33–35] where the impedance boundary conditions (i.e., the continuity of the tangential components of the electric and magnetic fields at the film interfaces) have been taken into account. Here we accomplish such calculations and give a classification of all of the branches in the spectrum of the eigenwaves in slabs of layered superconductors. We have found two types of eigenwaves. One of them is "true" surface modes, which decay exponentially from the slab boundaries. The second type of eigenwaves is waveguide modes (WGMs); their fields oscillate across the layers. The fields for both types of waves are evanescent outside the slab. We consider the case of a symmetric environment where the external dielectrics are the same. For this symmetric geometry, the eigenwaves are either symmetric or antisymmetric with respect to the central plane of the slab. As an example, we also study theoretically the problem of excitation of one of the waveguide modes by the attenuated-total-reflection method. For certain geometrical parameters, we predict an interesting effect of total suppression of the specular reflection due to the resonance excitation of the WGM.

II. FORMULATION OF THE EIGENVALUE PROBLEM AND DERIVATION OF THE DISPERSION EQUATION

Consider a slab of layered superconductor of thickness L clad between two nonmagnetic dielectrics with the same permittivity ε_d. The xy plane coincides with the crystallographic **ab** plane, and the z axis is along the crystallographic axis **c**. The plane $z = 0$ passes through the middle of the slab; see Fig. 1.

We search the eigenmodes of the transverse-magnetic (TM) polarization with the following components of the electric and magnetic fields:

$$\vec{E} = (E_x, 0, E_z), \quad \vec{H} = (0, H_y, 0). \tag{1}$$

The electromagnetic field inside a layered superconductor is related to the gauge-invariant phase difference $\varphi(x,z,t)$ of the order parameter in two neighboring layers. This phase difference is obtained from a set of coupled sine-Gordon equations (see, e.g., review 13, and references therein). For linear JPWs in the continuum limit, the phase $\varphi(x,z,t)$ can be excluded from the electrodynamic problem, which then can be reformulated in terms of an anisotropic frequency-dependent dielectric tensor with in-plane and out-of-plane components, $\varepsilon_{ab}(\omega)$ and $\varepsilon_c(\omega)$, respectively. In most practical cases, the thickness of the superconducting layers is much less than the thickness of the interlayer dielectrics. In this limit, the components $\varepsilon_{ab}(\omega)$ and $\varepsilon_c(\omega)$ have the following form:[36]

$$\varepsilon_c(\omega) = \varepsilon_s\left(1 - \frac{\omega_J^2}{\omega^2} + i\nu_c\frac{\omega_J}{\omega}\right),$$
$$\varepsilon_{ab}(\omega) = \varepsilon_s\left(1 - \frac{\omega_J^2}{\omega^2}\gamma^2 + i\nu_{ab}\frac{\omega_J}{\omega}\right). \tag{2}$$

Here, $\omega_J = (8\pi e D j_c/\hbar\varepsilon_s)^{1/2}$ is the Josephson plasma frequency, j_c is the maximum value of the Josephson current density $j_z = j_c \sin\varphi$, D is the spatial period of the layered structure, ε_s is the interlayer dielectric constant, $\gamma = \lambda_c/\lambda_{ab} \gg 1$ is the current-anisotropy parameter, and $\lambda_c = c/\omega_J\varepsilon_s^{1/2}$ and λ_{ab} are the magnetic-field penetration depths along and across the layers, respectively. The dimensionless relaxation frequencies $\nu_{ab} = 4\pi\sigma_{ab}/\varepsilon_s\omega_J$ and $\nu_c = 4\pi\sigma_c/\varepsilon_s\omega_J$ are proportional to the averaged quasiparticle conductivities σ_{ab} (along the layers) and σ_c (across the layers).

Equation (2) accounts for the inductive coupling between superconducting layers caused by the Josephson interlayer current. There exists also the capacitive mechanism of coupling, which is related to the violation of the electroneutrality condition.[37] The latter mechanism manifests itself in the dispersive characteristics of JPWs only in close vicinity to ω_J.[20] Here we study the dispersion equation for the SJPWs in a wide range of frequencies, therefore, in what follows, we neglect the capacitive mechanism of coupling.

We look for the magnetic field $H^s(x,z,t)$ of the TM eigenmodes in the slab in the form of a wave running along the x axis,

$$H^s(x,z,t) = A(z)\exp[i(qx - \omega t)]. \tag{3}$$

By substituting Eq. (3) into the Maxwell equations, we easily obtain the symmetric

$$A(z) = C_{\text{even}}\cos(k_s z) \tag{4}$$

and antisymmetric

$$A(z) = C_{\text{odd}}\sin(k_s z) \tag{5}$$

solutions with the transverse wave number

$$k_s^2 = \frac{1}{\lambda_c^2}(\Omega^2 - \gamma^2 + i\Omega\nu_{ab})\left(1 - \frac{\kappa^2}{\Omega^2 - 1 + i\Omega\nu_c}\right). \tag{6}$$

Here we introduced the dimensionless frequency $\Omega = \omega/\omega_J$ and the wave number $\kappa = q\lambda_c$.

It follows from Eqs. (4) and (5) that the structure of the eigenwaves in the transverse direction (along the z axis) is defined by the sign of the real part of k_s^2. If $\mathrm{Re}(k_s^2) > 0$, then the fields oscillate with coordinate z and the corresponding solution is a waveguide mode. In the opposite case, when

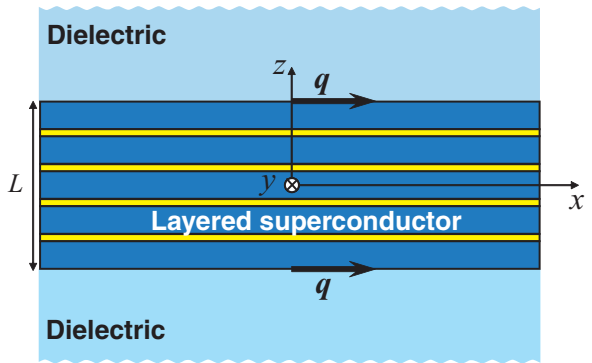

FIG. 1. (Color online) Geometry of the eigenvalue problem.

$\mathrm{Re}(k_s^2) < 0$, the fields decay exponentially from the slab boundaries. These solutions give rise to the surface modes. From Eq. (6), one can obtain the equations for curves in the (κ, Ω) plane that separate the regions of the surface and waveguide eigenmodes. If the dissipation is neglected, these equations have the following forms:

$$\Omega = 1, \quad \Omega = \gamma, \quad \Omega = \sqrt{1+\kappa^2}. \tag{7}$$

It is easy to see that the waveguide modes may exist in two different regions,

$$1 < \Omega < \gamma, \quad \kappa^2 > \Omega^2 - 1, \tag{8}$$

and

$$\Omega > \gamma, \quad \kappa^2 < \Omega^2 - 1. \tag{9}$$

Similarly, the surface modes may exist for

$$0 < \Omega < 1 \tag{10}$$

or

$$1 < \Omega < \gamma, \quad \kappa^2 < \Omega^2 - 1. \tag{11}$$

The separatrices given by Eq. (7) are shown by the thin red lines in Figs. 2, 3, and 4.

Knowing the magnetic component $H^s(x,z,t)$, it is easy to calculate, from the Maxwell equations, the electric fields. For the symmetric and antisymmetric modes, respectively, we derive

$$E_x^s(x,z,t) = -iC_{\mathrm{even}} \frac{k_s \lambda_c \Omega}{\sqrt{\varepsilon_s}} \frac{\sin(k_s z)}{\gamma^2 - \Omega^2 - i\Omega\nu_{ab}} \times \exp[i(qx - \omega t)], \tag{12}$$

$$E_x^s(x,z,t) = iC_{\mathrm{odd}} \frac{k_s \lambda_c \Omega}{\sqrt{\varepsilon_s}} \frac{\cos(k_s z)}{\gamma^2 - \Omega^2 - i\Omega\nu_{ab}} \exp[i(qx - \omega t)]. \tag{13}$$

The relation

$$E_z^s(x,z,t) = -H^s(x,z,t) \frac{\Omega\kappa}{\Omega^2 - 1 + i\Omega\nu_c} \tag{14}$$

between $E_z^s(x,z,t)$ and $H^s(x,z,t)$ has the same form for the symmetric and antisymmetric modes.

The fields above the slab decay exponentially and can be written as follows:

$$\begin{aligned} H^d(x,z,t) &= C_d \exp(iqx - i\omega t - k_d z), \\ E_x^d(x,z,t) &= iC_d \frac{\sqrt{\varepsilon_s}\lambda_c k_d}{\varepsilon_d \Omega} \exp(iqx - i\omega t - k_d z), \\ E_z^d &= -C_d \frac{\sqrt{\varepsilon_s}\kappa}{\varepsilon_d \Omega} \exp(iqx - i\omega t - k_d z), \end{aligned} \tag{15}$$

where the inverse decay length

$$k_d = \frac{1}{\lambda_c} \sqrt{\kappa^2 - \frac{\varepsilon_d}{\varepsilon_s}\Omega^2}. \tag{16}$$

The fields H^d and E_z^d below the slab for the symmetric (antisymmetric) modes are obtained by the symmetric (antisymmetric) reflection of the fields in Eq. (15). The component E_x^d is an odd (even) function of the coordinate z for the symmetric (antisymmetric) modes.

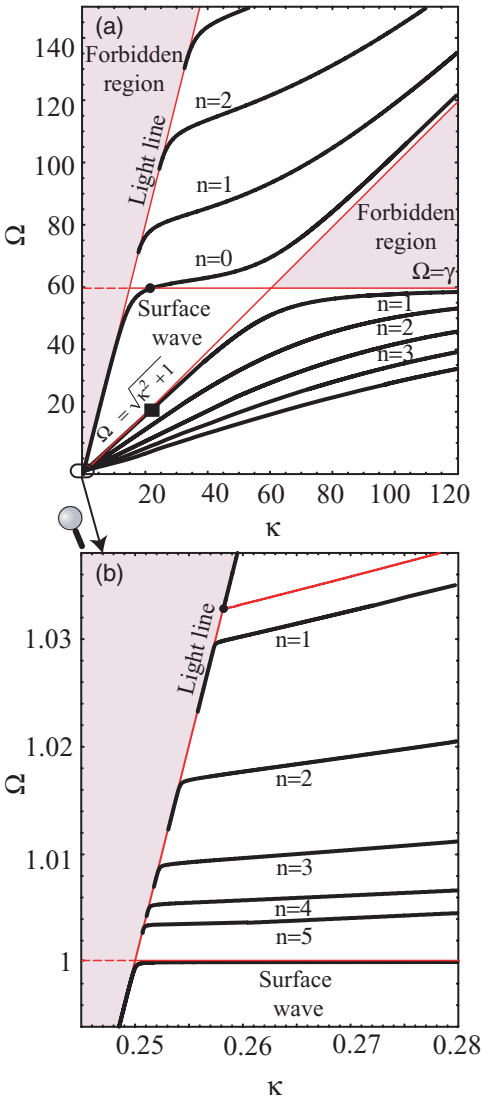

FIG. 2. (Color online) (a) Numerically calculated dispersion curves for the symmetric eigenmodes in a slab of layered superconductor placed in vacuum. Forbidden regions are shaded. The light line $\Omega = \sqrt{\varepsilon_s/\varepsilon_d}\kappa$ and the separatrices $\Omega = 1$, $\Omega = \gamma$, and $\Omega = \sqrt{1+\kappa^2}$ are shown by the thin red (grey) lines. (b) Close-up view of the region of low frequencies for the graph in (a). The plots are given for $\gamma \approx 60$, $\varepsilon_s = 16$, and $L/\lambda_{ab} = 10$.

The dispersion relation $\Omega(\kappa)$ for the eigenmodes is obtained by matching the impedance ratio E_x/H taken on both sides of the boundary $z = L/2$. This condition gives

$$\frac{k_d}{k_s} = \frac{\varepsilon_d}{\varepsilon_s} \frac{\Omega^2}{\Omega^2 - \gamma^2 + i\nu_{ab}\Omega} \tan\left(\frac{k_s L}{2}\right) \tag{17}$$

for the symmetric modes and

$$\frac{k_d}{k_s} = -\frac{\varepsilon_d}{\varepsilon_s} \frac{\Omega^2}{\Omega^2 - \gamma^2 + i\nu_{ab}\Omega} \cot\left(\frac{k_s L}{2}\right) \tag{18}$$

for the antisymmetric modes.

For extremely thick slabs, $L \to \infty$, Eqs. (17) and (18) become identical if the argument of the trigonometric functions is purely imaginary. In this case, the waves propagating

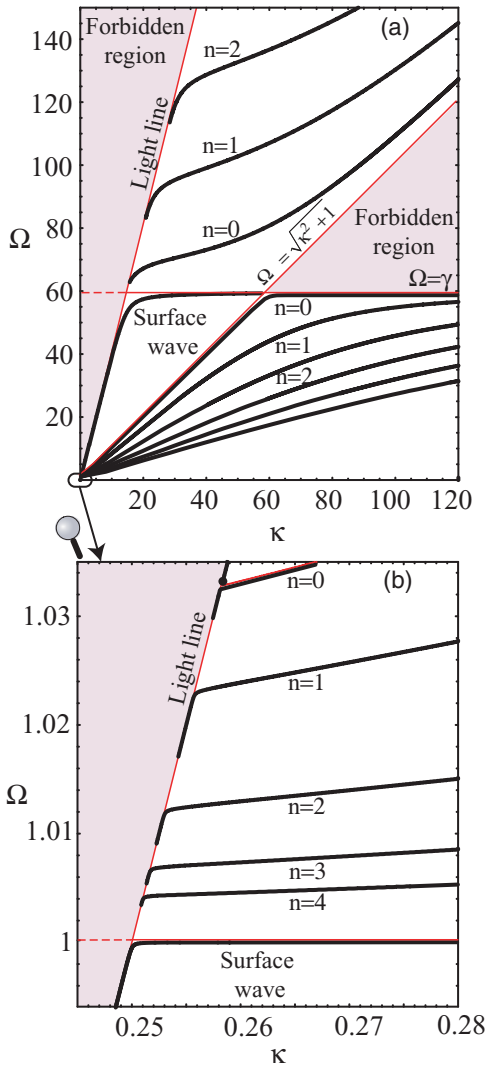

FIG. 3. (Color online) The same as in Fig. 2, but for the antisymmetric eigenmodes.

along both surfaces of the slab are decoupled. The symmetric and antisymmetric modes are transformed into independent surface Josephson plasma waves with the following dispersion relation:

$$\kappa(\Omega) = \sqrt{\frac{\varepsilon_d}{\varepsilon_s}}\,\Omega\left[\varepsilon_c(\Omega)\frac{\varepsilon_d - \varepsilon_{ab}(\Omega)}{\varepsilon_d^2 - \varepsilon_c(\Omega)\varepsilon_{ab}(\Omega)}\right]^{1/2}. \qquad (19)$$

This equation coincides with the dispersion relation for SJPWs in a semi-infinite layered superconductor.[27] We analyze the dispersion relations given by Eqs. (17) and (18) for the surface and waveguide modes in the next section.

III. ANALYSIS OF THE DISPERSION RELATIONS FOR SURFACE AND WAVEGUIDE MODES

All of the eigenmodes of the slab are evanescent, i.e., they decay exponentially in the surrounding external dielectrics. Therefore, according to Eq. (16), all of the dispersion curves should lie below the light line, $\Omega = (\varepsilon_s/\varepsilon_d)^{1/2}\kappa$, and the region above the light line is forbidden. The structure of the spectrum of the eigenmodes depends on the relation

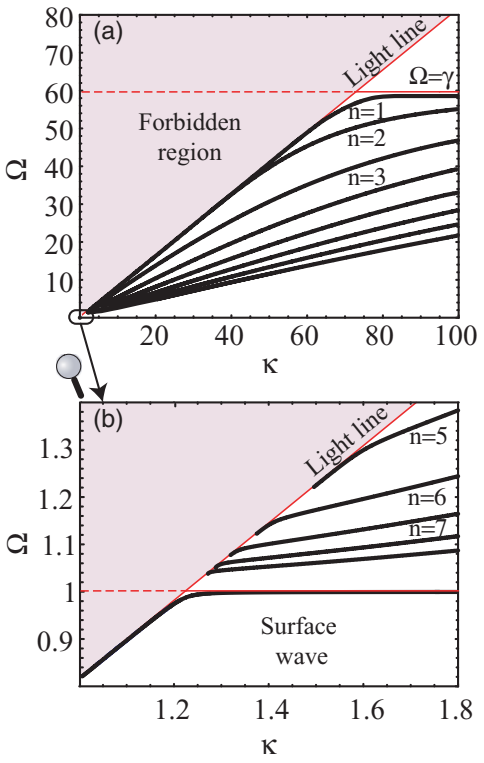

FIG. 4. (Color online) The same as in Fig. 2, but for the symmetric eigenmodes in a slab of layered superconductor placed between optically dense dielectrics.

between the permittivity ε_d of the external dielectrics and the permittivity ε_s of the interlayer constituent of the slab. Indeed, for optically soft external dielectrics,

$$\varepsilon_d < \varepsilon_s, \qquad (20)$$

both regions [given by Eqs. (10) and (11)] in the (κ, Ω) plane for SJPWs lie below the light line. In the opposite case of an optically dense environment,

$$\varepsilon_d > \varepsilon_s, \qquad (21)$$

the region given by Eq. (11) lies completely within the forbidden region, $\Omega > (\varepsilon_s/\varepsilon_d)^{1/2}\kappa$. Below we analyze the spectrum of the eigenmodes for the cases $\varepsilon_d < \varepsilon_s$ and $\varepsilon_d > \varepsilon_s$ separately. This analysis is done for a lossless medium.

A. Optically soft environment, $\varepsilon_d < \varepsilon_s$

1. Low-frequency surface waves, $\Omega < 1$

For low-frequency surface waves, $\Omega < 1$, the transverse wave number k_s given by Eq. (6) is purely imaginary,

$$k_s = \frac{i}{\lambda_{ab}}\sqrt{1 + \frac{\kappa^2}{1-\Omega^2}}, \qquad (22)$$

and the trigonometric functions in Eqs. (17) and (18) are replaced by the hyperbolic ones. Thus, the dispersion equations for low-frequency symmetric and antisymmetric SJPWs take the following form:

$$\frac{k_d}{|k_s|} = \frac{\varepsilon_d}{\varepsilon_s}\frac{\Omega^2}{\gamma^2}\tanh\left(\frac{|k_s|L}{2}\right), \qquad (23)$$

$$\frac{k_d}{|k_s|} = \frac{\varepsilon_d}{\varepsilon_s}\frac{\Omega^2}{\gamma^2}\coth\left(\frac{|k_s|L}{2}\right). \tag{24}$$

The dispersion curves given by Eqs. (23) and (24) start at $\kappa = \Omega = 0$, then follow the light line, deviating from it at Ω close to unity. For $\kappa \to \infty$, the slope of the dispersion curves tends to zero, and $\Omega(\kappa) \to 1$ with accuracy up to the terms $\sim 1/\gamma^2 \ll 1$. The numerical plots $\Omega(\kappa)$ for the low-frequency symmetric and antisymmetric SJPWs are shown in Figs. 2 (b) and 3(b).

2. *High-frequency surface waves,* $1 < \Omega < \gamma$

For the region of high-frequency surface waves, $1 < \Omega < \gamma$, the transverse wave number k_s given by Eq. (6) is purely imaginary if

$$\sqrt{\varepsilon_d/\varepsilon_s}\,\Omega < \kappa < \sqrt{\Omega^2 - 1}. \tag{25}$$

We obtain the following dispersion relations for the symmetric and antisymmetric high-frequency SJPWs, respectively:

$$\frac{k_d}{|k_s|} = \frac{\varepsilon_d}{\varepsilon_s}\frac{\Omega^2}{\gamma^2 - \Omega^2}\tanh\left(\frac{|k_s|L}{2}\right), \tag{26}$$

$$\frac{k_d}{|k_s|} = \frac{\varepsilon_d}{\varepsilon_s}\frac{\Omega^2}{\gamma^2 - \Omega^2}\coth\left(\frac{|k_s|L}{2}\right). \tag{27}$$

These dispersion curves start at the point with coordinates

$$\kappa_{\text{in}} = \sqrt{\frac{\varepsilon_d}{\varepsilon_s - \varepsilon_d}}, \quad \Omega_{\text{in}} = \sqrt{\frac{\varepsilon_s}{\varepsilon_s - \varepsilon_d}} > 1, \tag{28}$$

where the light line intersects with the hyperbola $\Omega = \sqrt{\kappa^2 + 1}$. Thus, there exists a gap

$$1 < \Omega < \sqrt{\frac{\varepsilon_s}{\varepsilon_s - \varepsilon_d}} \tag{29}$$

in the spectrum of the SJPWs in slabs of layered superconductors, which is similar to the case of semi-infinite samples.[27]

The spectrum of the symmetric high-frequency SJPWs ends at the point

$$\kappa_{\text{fin}} \approx \frac{\lambda_c \varepsilon_s}{L\varepsilon_d}\sqrt{2 + \frac{\varepsilon_d^2}{\varepsilon_s^2}\frac{L^2}{\lambda_{ab}^2} - 2\sqrt{1 + \frac{\varepsilon_d^2}{\varepsilon_s^2}\left(1 - \frac{\varepsilon_d}{\varepsilon_s}\right)\frac{L^2}{\lambda_{ab}^2}}}, \tag{30}$$

$$\Omega_{\text{fin}} = \gamma.$$

It is of interest that this ending point is simultaneously the starting point for one of the branches (with $n = 0$) of the high-frequency WGMs (the WGMs are discussed in the next section). In other words, the surface wave is continuously converted into the waveguide mode exactly in this point. This smooth transition is clearly seen in Fig. 2(a).

The ending point in the spectrum of the antisymmetric SJPWs lies on the hyperbola $\Omega = \sqrt{\kappa^2 + 1}$ at the frequency Ω_{fin},

$$\Omega_{\text{fin}} \approx \gamma\left(1 - \frac{\varepsilon_d \lambda_{ab}}{\sqrt{\varepsilon_s - \varepsilon_d}\,L}\right), \quad \lambda_{ab} \ll L. \tag{31}$$

The difference between Ω_{fin} and γ is proportional to λ_{ab}/L and it vanishes for a thick slab.

The numerical plots $\Omega(\kappa)$ for the high-frequency symmetric and antisymmetric SJPWs are shown in Figs. 2(a) and 3(a), respectively.

In the extremely thick slabs with $L \to \infty$, the surface waves propagate independently of each other along the upper and lower boundaries of a superconductor. For this case, the spectrum of SJPWs was studied in Refs. 22,25–27. The behavior of the dispersion curves for the low- and high-frequency surface waves in a slab of finite thickness is very similar to the case $L \to \infty$. The main difference is in the coordinates of the ending point in the spectrum; see Eqs. (30) and (31).

3. *Low-frequency waveguide modes,* $1 < \Omega < \gamma$

In the region of low-frequency waveguide modes, $1 < \Omega < \gamma$, the transverse wave number k_s given by Eq. (6) is real and positive for

$$\kappa > \sqrt{\Omega^2 - 1}. \tag{32}$$

This condition corresponds to the waveguide eigenmodes with fields oscillating across the slab thickness. The ratio k_d/k_s on the left-hand sides of Eqs. (17) and (18) is positive. Then, the argument $k_s L/2$ of the trigonometric functions in these equations is allowed to vary within the intervals

$$\pi(2n-1)/2 < k_s L/2 < \pi n, \quad n = 1,2,3\ldots, \tag{33}$$

for the symmetric waveguide modes, and within

$$\pi n < k_s L/2 < \pi(2n+1)/2, \quad n = 0,1,2\ldots, \tag{34}$$

for the antisymmetric ones. Here, n enumerates different branches of the waveguide modes.

Each branch of the $\Omega_n(\kappa)$ curve starts from the light line at the frequency $\Omega = \Omega_{\text{in}}^{(n)}$, where

$$1 < \Omega_{\text{in}}^{(n)} < \sqrt{\frac{\varepsilon_s}{\varepsilon_s - \varepsilon_d}}. \tag{35}$$

Note that the frequency interval given by Eq. (35) where the branches $\Omega_n(\kappa)$ start coincides exactly with the frequency gap given by Eq. (29) in the spectrum of the surface waves.

For $\kappa \to \infty$, all of the dispersion curves $\Omega^{(n)}(\kappa)$ of the waveguide modes tend to γ [see Figs. 2(a) and 3(a)]. The distances between the dispersion curves diminish as n increases. The dispersion curves become more crowded approaching the line $\Omega = 1$.

4. *High-frequency waveguide modes,* $\Omega > \gamma$

The waveguide modes can propagate in this high-frequency range ($\Omega > \gamma$) if $\sqrt{\varepsilon_d/\varepsilon_s}\,\Omega \leqslant \kappa < \sqrt{\Omega^2 - 1}$. The right-hand sides of Eqs. (17) and (18) are positive if the argument $k_s L/2$ of the trigonometric functions in these equations lies within the intervals

$$\pi n < k_s L/2 < \pi(2n+1)/2, \quad n = 0,1,2\ldots, \tag{36}$$

for the symmetric waveguide modes, and within

$$\pi(2n+1)/2 < k_s L/2 < \pi(n+1), \quad n = 0,1,2\ldots, \tag{37}$$

for the antisymmetric ones.

All of the dispersion curves, except the one for the symmetric mode with $n = 0$, start from the light line and asymptotically tend to the limiting value $\Omega = \kappa$ at $\kappa \to \infty$ [see Figs. 2(a) and 3(a)]. The dispersion curve for the symmetric mode with $n = 0$ starts at the point ($\kappa = \kappa_{\rm fin}$, $\Omega = \gamma$), which is the ending point for the high-frequency surface mode. The value of $\kappa_{\rm fin}$ is given by Eq. (30).

B. Optically dense environment, $\varepsilon_d > \varepsilon_s$

In an optically dense environment, $\varepsilon_d > \varepsilon_s$, the separatrix $\Omega = \sqrt{1+\kappa^2}$ passes through the forbidden region $\Omega > (\varepsilon_s/\varepsilon_d)^{1/2}\kappa$ (see Fig. 4). Therefore, contrary to the case of an optically soft environment, there exists only one region for the surface waves in the (κ, Ω) plane [Eq. (10)] and only one region for the waveguide modes,

$$1 < \Omega < \gamma, \quad \kappa > (\varepsilon_d/\varepsilon_s)^{1/2}\Omega. \tag{38}$$

The plots of the dispersion curves for the SJPWs and WGMs are similar to the low-frequency branches of the spectrum shown in Figs. 2 and 3 for the case of $\varepsilon_d < \varepsilon_s$. These curves for the symmetric modes are presented in Fig. 4.

In the case of relatively small frequencies, for $\Omega \ll \gamma$, the dispersion relations for the waveguide modes can be written as follows:

$$\begin{aligned} \frac{k_d}{k_s} &= m\varepsilon_d k^2 \lambda_{ab}^2 \tan^m\left(\frac{k_s L}{2}\right), \\ k_s &= \frac{1}{\lambda_{ab}}\sqrt{1-\frac{\kappa^2}{\Omega^2-1}}, \end{aligned} \tag{39}$$

with $m = -1$ for symmetric modes and $m = 1$ for antisymmetric ones. This result was reported in Refs. 33–35.

IV. EXCITATION OF A WAVEGUIDE JOSEPHSON PLASMA MODE

It is known that the excitation of surface waves in metal slabs may be accompanied by anomalous resonance phenomena in the reflectivity and transmissivity (see, e.g., Refs. 38–40). In particular, complete suppression of the specular reflection can be observed for some specific parameters of the system. In this section, we discuss the excitation of a waveguide mode in a slab of layered superconductor and show that the specular reflection of the incident terahertz wave can be completely suppressed.

We consider the excitation of the symmetric low-frequency waveguide mode with number $n = 1$ in a slab placed in vacuum. The wave vector and the frequency of the excited wave are marked by black filled square in Fig. 2(a). This mode can be excited via the so-called attenuated-total-reflection method (Otto configuration).[41] Two waves incident symmetrically from two identical dielectric prisms onto boundaries of a superconducting slab. The slab is separated from the prisms by two thin vacuum gaps (see Fig. 5). In the absence of the superconductor, the incident waves completely reflect from the bottoms of the prisms if the incident angle θ exceeds the critical angle $\theta_t = \arcsin(1/\sqrt{\varepsilon_p})$, corresponding to the total internal reflection (here, ε_p is the dielectric constant of the prisms). However, the evanescent waves penetrate into the vacuum gaps

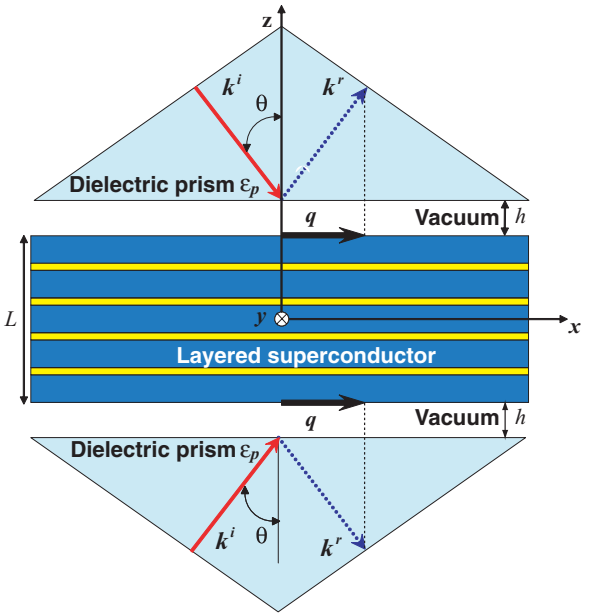

FIG. 5. (Color online) Geometry of excitation of symmetric eigenmodes by the "attenuated-total-reflection" method. Here, $\mathbf{k}^i$ and $\mathbf{k}^r$ are the wave vectors of the incident and reflected waves, respectively.

at a distance of about the wavelength. The wave vectors of the evanescent modes are directed along the surfaces of the prisms. The modulus of each wave vector exceeds ω/c. The same is true for the wave vectors of the surface and waveguide modes. So, the matching conditions for the frequencies and the wave vectors of the evanescent waves and the waveguide Josephson plasma mode can be satisfied for a certain incident angle. Under the condition of resonant excitation of the WGM, the effect of *strong suppression of reflected waves* can be observed.

Due to the symmetry of the problem, it is sufficient to find the spatial distribution of the electromagnetic field for semispace $z > 0$ (above the central plane of the slab) and the coefficient R of reflection from the boundary $z = L/2 + h$ of the upper prism. Here, h is the thickness of the vacuum gap. The dimensionless magnetic field H^p in the prism (for $z > L/2 + h$) is a sum of the fields of the incident and specularly reflected waves,

$$\begin{aligned} H^p &= \exp(-i\omega t + iqx - ik_p z) \\ &\quad + R\exp(-i\omega t + iqx + ik_p z). \end{aligned} \tag{40}$$

The longitudinal and transverse components, q and k_p, of the wave vector in the prism are

$$q = \frac{\omega\sqrt{\varepsilon_p}}{c}\sin\theta, \quad k_p = \frac{\omega\sqrt{\varepsilon_p}}{c}\cos\theta, \tag{41}$$

where θ is the angle of incidence exceeding $\arcsin(1/\sqrt{\varepsilon_p})$.

The magnetic field H^v in the vacuum gap is a sum of two evanescent waves,

$$\begin{aligned} H^v &= h^+\exp(-i\omega t + iqx + k_v z) \\ &\quad + h^-\exp(-i\omega t + iqx - k_v z). \end{aligned} \tag{42}$$

The spatial decrement k_v is defined as

$$k_v = \frac{\omega}{c}\sqrt{\varepsilon_p \sin^2\theta - 1}. \tag{43}$$

The magnetic field H^s in the superconductor has the form

$$H^s = C\cos(k_s z)\exp(-i\omega t + iqx), \tag{44}$$

with the transverse wave number k_s given by Eq. (6).

Using the Maxwell equations and Eqs. (40), (42), and (44), we can easily derive the tangential components E_x^p, E_x^v, and E_x^s of the electric field in the prism, vacuum, and layered superconductor, respectively,

$$E_x^p = -\frac{k_p c}{\omega\varepsilon_p}[\exp(-i\omega t + iqx - ik_p z) - R\exp(-i\omega t + iqx + ik_p z)], \tag{45}$$

$$E_x^v = -\frac{ik_v c}{\omega}[h^+\exp(-i\omega t + iqx + k_v z) - h^-\exp(-i\omega t + iqx - k_v z)], \tag{46}$$

$$E_x^s = -iC\frac{\Omega k_s \lambda_c}{\sqrt{\varepsilon_s}(\gamma^2 - \Omega^2 - i\Omega\nu_{ab})}\sin(k_s z) \times \exp(-i\omega t + iqx). \tag{47}$$

The continuity conditions for the fields H and E_x at the interfaces $z = L/2$ and $z = L/2 + h$ give four linear equations for the unknown field amplitudes R, h^+, h^-, and C. Solving these equations, after some algebra, we obtain the reflectivity coefficient R,

$$R = \frac{k_p[k_v + \alpha\tanh(k_v h)] - i\varepsilon_p k_v[\alpha + k_v\tanh(k_v h)]}{k_p[k_v + \alpha\tanh(k_v h)] + i\varepsilon_p k_v[\alpha + k_v\tanh(k_v h)]} \times \exp[-ik_p(L + 2h)], \tag{48}$$

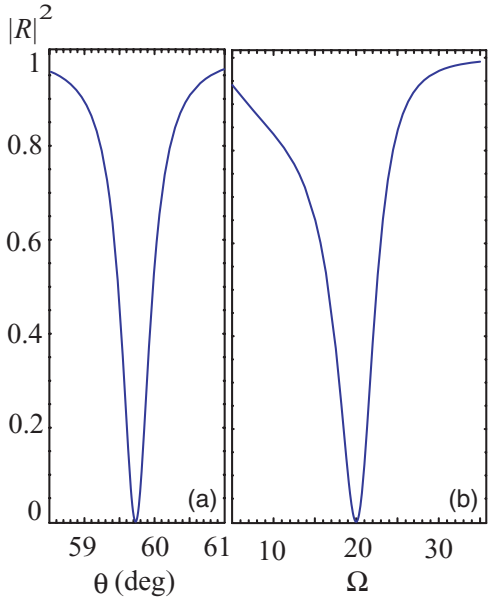

FIG. 6. (Color online) Reflectivity $|R|^2$ as a function of (a) the incidence angle θ for given $\Omega = 20$, and (b) the frequency Ω for given $\theta = 59.7^\circ$. These resonant values of θ and Ω determine a point on the dispersion curve in the (κ, Ω) plane. In Fig. 2, this point is marked by black filled square on the dispersion curve with $n = 1$. The optimal thickness of the vacuum gap is $h = 0.28\lambda_{ab}$. Other parameters are $\gamma = 60$, $\varepsilon_s = 16$, $L/\lambda_{ab} = 10$, $\varepsilon_p = 24$, and $\nu_{ab} = \nu_c = 5 * 10^{-2}$.

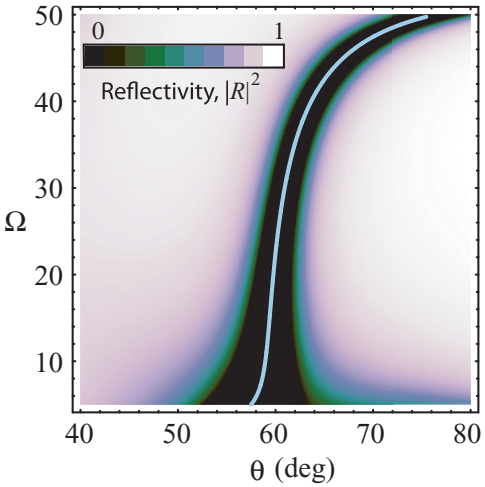

FIG. 7. (Color online) The intensity plot of the reflectivity $|R|^2$ in the (θ, Ω) plane for the same values of the parameters as in Fig. 6. The dispersion curve for the symmetric low-frequency waveguide mode with $n = 1$ is shown by the light-blue line in the center of the figure.

with

$$\alpha = \frac{\Omega^2 k_s \lambda_{ab}\tan(k_s L/2)}{\varepsilon_s(\gamma^2 - \Omega^2 - i\Omega\nu_{ab})}.$$

The coupling of the waves in the prism and superconductor results in the breaking of the total internal reflection. Indeed, the parameter α in Eq. (48) is not purely real if $\nu_c, \nu_{ab} \neq 0$. Therefore, the modulus of the reflectivity coefficient, $|R|$, is less than one. This means that reflectivity is suppressed due to the excitation of the waveguide mode in the slab of layered superconductor. Moreover, under the resonance conditions, both the real and imaginary parts of the numerator in Eq. (48) can simultaneously vanish at an appropriate choice of the thickness $h_{\rm opt}$ of the vacuum gaps. Thus, for a given frequency, the resonant value of the incidence angle and the optimal gap thickness $h_{\rm opt}$ can be obtained by equating the numerator in Eq. (48) to zero.

The complete suppression of the specular reflectivity can be observed for the optimal gap thickness either by changing the incidence angle θ at a given frequency Ω, or, vice versa, by changing the frequency Ω at a given incidence angle θ. An example of complete suppression is shown in Figs. 6(a) and 6(b), where we plot the functions $|R(\theta)|^2$ and $|R(\Omega)|^2$, respectively. An intensity plot of the reflectivity in the (θ, Ω) plane is shown in Fig. 7. Each point on the dispersion curve (light-blue line) gives a pair of parameters (the incident angle and the frequency) for which the total internal reflection is completely suppressed.

V. CONCLUSIONS

Here we presented a systematic study of the dispersion properties of the surface and waveguide eigenmodes in a slab of layered superconductor placed between two identical dielectrics. The structure of the eigenspectrum depends on the relation between the dielectric constants of the environment and the insulator separating the superconducting layers. For the case of an optically soft environment, we show that

there are two symmetric and two antisymmetric branches of surface waves. The fields of these waves are concentrated near the slab boundaries and decay exponentially away from them. In addition, the spectrum contains an infinite number of low- and high-frequency waveguide eigenmodes. These modes oscillate across the slab thickness. For the case of an optically dense environment, the high-frequency branches vanish and the spectrum consists of only the low-frequency branches of the surface and waveguide modes. Since the spectrum of the eigenfrequencies fits the terahertz region, the layered superconductors may find useful applications as effective waveguides for terahertz radiation.

We show that the eigenmodes can be resonantly excited in a slab by means of the attenuated-total-reflection method. Weak coupling of the external electromagnetic wave with one of the eiegenmodes occurs through the evanescent tail of the wave, which is reflected from the bottom of a prism. For a given frequency, the conditions of the resonant coupling are satisfied for a specific angle of incidence. We predict that the resonant coupling may be sufficient to completely suppress the reflected wave. This effect can be observed for the optimal thickness of the vacuum gap between the prism and the slab. For this special configuration of the parameters, the energy of the incident wave is completely dissipated in the slab. This phenomenon is analogous to the well-known Wood anomaly, which is related to surface-plasmon polariton resonance in the visible and near-infrared region.

ACKNOWLEDGMENTS

We gratefully acknowledge partial support from the US Department of Energy Grant No. DE-FG02-06ER46312, from the Ukrainian State program "Nanotechnologies and nanomaterials," and from the program of NASU "Fundamental problems of nanostructures, nanomaterials and nanotechnologies" (Grant No. 9/11-H).

[1] T. W. Ebbesen, H. J. Lezec, H. F. Ghaemi, T. Thio, and P. A. Wolff, Nature (London) **391**, 667 (1998).
[2] H. A. Bethe, Phys. Rev. **66**, 163 (1944).
[3] A. V. Zayats, I. I. Smolyaninov, and A. A. Maradudin, Phys. Rep. **408**, 131 (2005).
[4] I. S. Spevak, A. Yu. Nikitin, E. V. Bezuglyi, A. Levchenko, and A. V. Kats, Phys. Rev. B **79**, 161406 (2009).
[5] J. B. Pendry, L. Martin-Moreno, and F. J. Garcia-Vidal, Science **305**, 847 (2004).
[6] K. Wang and D. Mittleman, Nature (London) **432**, 376 (2004).
[7] K. Wang and D. Mittleman, J. Opt. Soc. Am. B **22**, 2001 (2005).
[8] T.-I. Jeon, J. Zhang, and D. Grischkowsky, Appl. Phys. Lett. **86**, 161904 (2005).
[9] A. Nahata, W. Zhu, and A. Agrawal, Opt. Express **16**, 6216 (2008).
[10] T. H. Isaac, W. L. Barnes, and E. Hendry, Appl. Phys. Lett. **93**, 241115 (2008).
[11] R. Kleiner, F. Steinmeyer, G. Kunkel, and P. Muller, Phys. Rev. Lett. **68**, 2394 (1992).
[12] R. Kleiner and P. Muller, Phys. Rev. B **49**, 1327 (1994).
[13] S. Savel'ev, V. A. Yampol'skii, A. L. Rakhmanov, and F. Nori, Rep. Prog. Phys. **73**, 026501 (2010).
[14] L. N. Bulaevskii, M. Zamora, D. Baeriswyl, H. Beck, and J. R. Clem, Phys. Rev. B **50**, 12831 (1994).
[15] S. E. Shafranjuk, M. Tachiki, and T. Yamashita, Phys. Rev. B **55**, 8425 (1997).
[16] M. Tachiki, T. Koyama, and S. Takahashi, Phys. Rev. B **50**, 7065 (1994).
[17] L. N. Bulaevskii, M. P. Maley, and M. Tachiki, Phys. Rev. Lett. **74**, 801 (1995).
[18] M. Machida, T. Koyama, and M. Tachiki, Physica C **341**, 1385 (2000).
[19] Ch. Helm, L. N. Bulaevskii, E. M. Chudnovsky, and M. P. Maley, Phys. Rev. Lett. **89**, 057003 (2002).
[20] L. N. Bulaevskii, Ch. Helm, A. R. Bishop, and M. P. Maley, Europhys. Lett. **58**, 415 (2002).
[21] Ch. Helm and L. N. Bulaevskii, Phys. Rev. B **66**, 094514 (2002).
[22] S. Savel'ev, V. Yampol'skii, and F. Nori, Phys. Rev. Lett. **95**, 187002 (2005).
[23] S. Savel'ev, V. Yampol'skii, A. L. Rakhmanov, and F. Nori, Physica C **445-448**, 183 (2006).
[24] S. Savel'ev, V. Yampol'skii, A. Rakhmanov, and F. Nori, Physica C **437-438**, 281 (2006).
[25] V. A. Yampol'skii, A. V. Kats, M. L. Nesterov, A. Yu. Nikitin, T. M. Slipchenko, S. Savel'ev, and F. Nori, Phys. Rev. B **76**, 224504 (2007).
[26] V. A. Yampolskii, A. V. Kats, M. L. Nesterov, A. Yu. Nikitin, and T. M. Slipchenko, Phys. Rev. B **79**, 214501 (2009).
[27] V. A. Golick, D. V. Kadygrob, V. A. Yampolskii, A. L. Rakhmanov, B. A. Ivanov, and F. Nori, Phys. Rev. Lett. **104**, 187003 (2010).
[28] V. M. Krasnov and D. Winkler, Phys. Rev. B **56**, 9106 (1997).
[29] V. M. Krasnov, Phys. Rev. B **60**, 9313 (1999).
[30] V. M. Krasnov and D. Winkler, Phys. Rev. B **60**, 13179 (1999).
[31] N. F. Pedersen and S. Sakai, Phys. Rev. B **58**, 2820 (1998).
[32] V. M. Krasnov, Phys. Rev. B **63**, 064519 (2001).
[33] M. M. Doria, F. Parage, and O. Buisson, Europhys. Lett. **35**, 445 (1996).
[34] M. M. Doria, G. Hollauer, F. Parage, and O. Buisson, Phys. Rev. B **56**, 2722 (1997).
[35] M. M. Doria, Flávio M. R. dAlmeida, and O. Buisson, Phys. Rev. B **57**, 5489 (1998).
[36] A. L. Rakhmanov, V. A. Yampol'skii, J. A. Fan, F. Capasso, and F. Nori, Phys. Rev. B **81**, 075101 (2010).
[37] T. Koyama and M. Tachiki, Phys. Rev. B **54**, 16183 (1996).
[38] V. M. Agranovich and D. L. Mills, *Surface Polaritons* (Nauka, Moscow, 1985).
[39] H. Raether, *Surface Plasmons* (Springer-Verlag, New York, 1988).
[40] R. Petit, *Electromagnetic Theory of Gratings* (Springer, Berlin, 1980).
[41] A. Otto, Z. Phys. **216**, 398 (1968).